ROSAT HRI Observations of M31 supernova remnants

Magnier, E.A.; Primini, F.A.; Prins, S.; van Paradijs, J.A.; Lewin, W.H.G.

Published in:
Astrophysical Journal

DOI:
10.1086/304917

THE ASTROPHYSICAL JOURNAL, 490:649–652, 1997 December 1

ROSAT HRI OBSERVATIONS OF M31 SUPERNOVA REMNANTS

EUGENE A. MAGNIER
Astronomy Department 351580, University of Washington, Seattle, WA 98195; gene@astro.washington.edu
FRANCIS A. PRIMINI[1]
Physics Department, 376 Weniger Hall, Oregon State University, Corvalis, OR 97331
SASKIA PRINS[2] AND JAN VAN PARADIJS[3]
Astronomical Institute "Anton Pannekoek" and Center for High Energy Astrophysics, University of Amsterdam, Kruislaan 403, 1098 SJ Amsterdam, The Netherlands
AND
WALTER H. G. LEWIN
Massachusetts Institute of Technology, 37-624, Cambridge, MA 02139
Received 1997 April 30; accepted 1997 July 15

ABSTRACT

We have observed M31 using the *ROSAT* HRI. We have searched for X-ray emission from supernova remnants (SNRs) previously identified from surveys using narrowband optical observations. We find that a surprisingly small number of the identified SNRs are detected in X-rays at a threshold of $\approx 10^{35}$ ergs s^{-1}. The absence of detected X-ray flux from many of the optically identified SNRs suggests that the local ISM density in the vicinity of these SNRs is typically quite low, less than 0.1 cm^{-3}. The few that have been detected likely represent the upper end of the density distribution, having implied ambient densities in the range 0.1 to >10 cm^{-3}. Since H I observations show that all SNRs are in regions with large column densities, which implies densities of 1–10 cm^{-3}, a multicomponent ISM must be invoked. Our measured densities are upper limits for the dominant low-density component of the ISM.

Subject headings: galaxies: individual (M31) — galaxies: ISM — supernova remnants — X-rays: ISM

1. INTRODUCTION

The nearby large spiral galaxy M31 is an ideal location in which to study global properties of supernova remnant (SNR) populations. It is close, massive, and similar in many respects to the Milky Way. It has active star formation so that Type II SNRs are expected. Most importantly, though, SNRs in M31 are all at the same, well-known distance of ≈ 710 kpc (Welch et al. 1986). The work of Berkhuijsen (1986) highlighted the importance of a sample of SNRs for which the distance is known, but it also showed the limited depth of existing samples of SNRs. We have been studying the M31 SNR population using observations in a variety of wavelength regimes. Here we report on X-ray observations of SNRs in the northeast disk regions of M31 and the implications for the ISM conditions in the vicinity of the SNRs.

2. OBSERVATIONS

The *ROSAT* HRI is an X-ray imager with sensitivity in the range 0.02–2.5 keV and spatial resolution $\approx 6''$ in the center to $30''$ near the edge of the $\approx 30'$ field of view. We used the HRI to observe a portion of the disk of M31 northeast of the core. This region was observed in two periods, from 10:53 UT 1996 January 21 to 19:11 UT 1996 February 5 (≈ 70 ks) and from 13:09 UT 1996 July 7 to 23:57 UT 1996 July 8 (≈ 165 ks). After processing, the total exposure time was 237,363 s. The source detection was performed in two independent ways. First, a $12'' \times 12''$ box was moved across the raw image, and sources were identified if they had a signal-to-noise ratio in the box greater than 3. Second, the raw image was smoothed with a Gaussian of FWHM $9''$. The smoothed image was inspected by eye for any sources that stood out above the background variations. These two methods agreed very well, producing nearly identical lists, with 62 sources in the first and 58 sources in the second. A future paper will discuss in detail the properties of the detected sources, including a discussion of the variability between the epochs of the two observations. In this paper we will discuss only the detection of SNRs.

We have calculated X-ray luminosities for the sources using a constant conversion factor from HRI counts s^{-1} to ergs s^{-1}. Since the HRI has no spectral resolution, we have assumed a Raymond-Smith emission spectrum with $kT = 0.86$ keV and extinction corresponding to $N_H = 10^{21}$ cm^{-2}, which is typical for an SNR. We have also examined the effect on the predicted luminosities if the temperature varied from 0.086 to 3.43 keV. The largest error we would make would be for low temperatures, where our predicted luminosity would be 35% too low. The Raymond-Smith models assume local thermal equilibrium (LTE). We have also examined the effects of non-LTE models by Hamilton, Sarazin, & Chevalier (1983) on the predicted luminosity. In some cases, there may be an error of up to a factor of 5 in luminosity (predicted luminosities too high). Below we discuss the implication of these errors.

We have compared the X-ray source positions with optically identified SNR candidates from the three major catalogs: Blair, Kirshner, & Chevalier (1981), Braun & Walterbos (1993), and Magnier et al. (1995). We will use their names for the optical SNRs. The HRI field of view includes 91 SNRs, 67 within the inner $30'$. Seven optical SNRs are coincident with six distinct X-ray sources. Of these, three (BA 521, K446, and K583) are also consistent with other possible optical counterparts (e.g., globular clusters, blue stars), making the association less certain. Two (2-033 and 3-057) are associated with a single X-ray source.

[1] Also at the Smithsonian Astrophysical Observatory.
[2] Also at the Isaac Newton Group, Canary Islands.
[3] Also at the Physics Department, University of Alabama in Huntsville.

The remaining two optical SNRs are 2-048 and 3-059 (BA 055). It is clear that only a small fraction ($\lesssim 7\%$) of the optically identified SNRs are detected in the X-rays. We will now consider possible selection effects that may inhibit the X-ray detections.

One possibility is that the list of optically identified SNRs includes many false identifications. The Magnier et al. (1995) catalog of SNRs includes a "quality" classification consisting of three levels. There is no tendency for the X-ray–identified SNRs to be high-quality candidates: two have a medium quality, two have a low quality, and none have a high quality. For that matter, only three of the 30 Braun & Walterbos (1993) SNRs in this field are detected in X-rays. These SNRs have a generally high quality as they needed both high [S II]/Hα as well as radio continuum emission to be identified. The fact that a high fraction (three of four) of the Blair et al. (1981) SNRs are detected probably reflects the general correlation between the X-ray and Hα surface brightnesses.

Another possible selection effect is X-ray absorption. However, model X-ray spectra including foreground absorption show that the X-ray flux is significantly diminished only when the absorption reaches a level corresponding to $N_{\rm H} = 3 \times 10^{22}$ cm^{-2}, which is equivalent to an optical extinction of $A_V = 19.4$ (Bohlin, Savage, & Drake 1978). Thus, we expect the optical emission to be more strongly affected by extinction than the X-rays. Since all of our SNRs are optically detected, their optical extinction cannot be very large ($\lesssim 1$ mag). In fact, if the extinction is due to locally higher ISM densities, then the selection effect is opposite from one's intuition: SNRs that occur in denser media, where the extinction is higher, should be *brighter* in X-rays for a given diameter, not fainter. The increased luminosity generated in the interaction with the ISM compensates for the absorption from the ISM. We conclude that the lack of X-ray detections is not due to a selection effect, but rather to intrinsically faint X-ray emission from the SNRs. We will now discuss the implications of the faint X-ray emission.

3. Σ_X-D RELATION

Figure 1 shows the X-ray surface brightness (Σ_X) versus the radio diameter (D) for SNRs with known distance in the Galaxy, LMC, and SMC. The SNRs from our M31 observations are included using the optical diameter. Our three X-ray sources with other possible optical counterparts are also marked with a cross, and the two optical SNRs identified with one X-ray source are circled. The data for the SNRs in the Galaxy and Magellanic Clouds are taken from the compilation of Berkhuijsen (1986): all SNRs in this compilation with X-ray fluxes were included. We include in this plot a line to represent the 2 σ detection limit of our HRI observations. At the bottom of the figure is the size distribution for the 91 optically identified SNRs in our field of view.

The X-ray surface brightness and diameter of a remnant is principally related to the local ISM density and the initial energy of the explosion. We have used models based on Fusco-Femiano & Preite-Martinez (1984) for comparison with our observations. The X-ray luminosity of the SNR can simply be described by

$$L_{\rm X} = \bar{\Lambda} n_0^2 V \,, \tag{1}$$

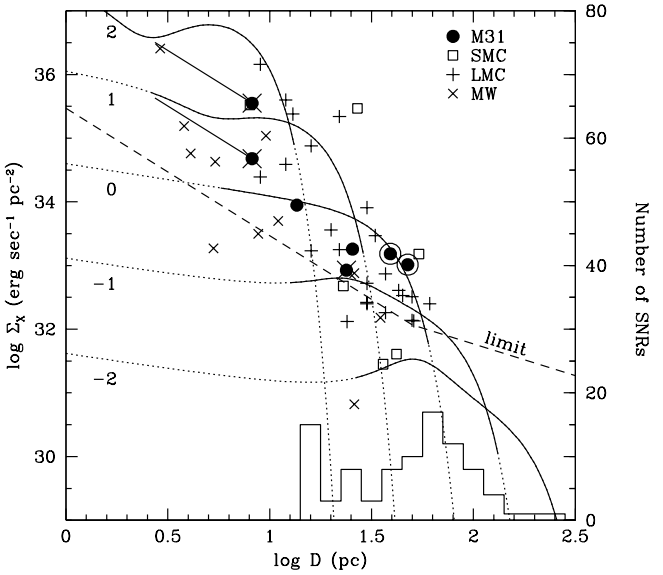

FIG. 1.—Diameter vs. X-ray surface brightness for SNRs in M31, the Milky Way, and the Magellanic Clouds. Different point types represent SNRs in different galaxies. The smooth curves represent evolution models for SNRs with different ambient densities, labeled by the logarithm of the density in cm^{-3} (see text for details). The diagonal lines represent the completeness limit and detection limit for our *ROSAT* HRI observations. The histogram represents the diameter distribution of the optically identified SNRs in our HRI field. The corresponding number is given on the right-hand axis.

where V is the total volume of the SNR, and $\bar{\Lambda}$ is the mean emissivity in the energy band of interest determined over the radial distribution of the gas density, normalized to the ambient density, n_0. For SNR temperatures that are high compared to the low-energy end of the detector, much of the flux is dominated by line emission, and $\bar{\Lambda}$ must be calculated in detail. For low temperatures, the in-band flux is dominated by thermal continuum emission and $\bar{\Lambda}$ can then be calculated analytically. In the low-temperature regime,

$$\bar{\Lambda} \approx 3T^{0.5} e^{-E_{\rm lo}/T} \,, \tag{2}$$

where $E_{\rm lo}$ is the lower energy bound on the detector (≈ 0.1 keV for the HRI), T is the temperature in keV, and $\bar{\Lambda}$ is in units of 10^{-23} ergs cm^3 s^{-1}. For the high-temperature regime, $\bar{\Lambda}$ has been calculated by Fusco-Femiano & Preite-Martinez (1984) for models of LMC SNRs in the adiabatic phase. The form of $\bar{\Lambda}$ varies only a small amount ($\approx 50\%$) from the thermal limit and depends on both the density and the initial energy of the explosion, characterized by the parameter $\eta = n_0^2 E_{51}$, where E_{51} is the energy of the explosion in units of 10^{51} ergs. The form of $\bar{\Lambda}$ in their models is shown in their Figure 2. We have used an analytical approximation to represent the logarithmic difference from the thermal limit, $\log \bar{\Lambda} = \log \bar{\Lambda}_{\rm thermal} + \Delta \log \bar{\Lambda}$. We have used

$$\Delta \log \bar{\Lambda} = \frac{-0.2 \log n_0}{1 + 1.5(\log T - 0.5)^2} \,, \tag{3}$$

which fits reasonably well within the range of their models. Since $\Delta \log \bar{\Lambda}$ makes a shift in $\log \Sigma_{\rm X}$ of only 0.5 at the extremes, the accuracy of this analytical representation is sufficient for the effects we are investigating.

We are interested in the variations of the surface brightness, $\Sigma_{\rm X} = 4L_{\rm X}/\pi D^2$, with the diameter, D. The Sedov simi-

larity solutions (Sedov 1959) allow us to connect the SNR diameter with the temperature of the gas for the adiabatic phase: $T = 4900 E_{51}\ D^{-3} n_0^{-1}$, where T is in keV, D is in parsecs, and n_0 is in cm^{-3}. Combining equations (1), (2), and (3), converting luminosity to surface brightness, and making the appropriate unit adjustments, we find

$$\Sigma_X = 10^{34.6}\,\delta\Lambda n_0^{1.5} D^{-0.5} e^{-E_{51}(D/17)^3(n_0/E_{51})}\ , \qquad (4)$$

where $\delta\Lambda = 10^{\log \Delta\Lambda}$ and Σ_X is in ergs s^{-1} pc^{-2}. We have plotted evolution tracks using equation (4) on Figure 1 assuming $E_{51} = 1$. We have used a dotted line to represent the periods before and after the adiabatic phase. Before the remnant reaches the adiabatic phase, the expansion is faster making the tracks flatter than shown. After the adiabatic phase, the expansion slows, and the tracks should fall more quickly than shown. The curves are labeled with the logarithm of the density, n_0.

4. AMBIENT DENSITY

We can use Figure 1 to estimate the ambient density for the SNRs in our sample. For an SNR with a given diameter and X-ray surface brightness, there is a degeneracy between a high-density and a low-density track. However, except at the outer boundary of the tracks, the high-density track is well into the radiative phase when it crosses the low-density track. At this point, the shock velocity is expected to be quite low, which makes it unlikely to be detectable optically, and the remnant cools quickly, which makes the observable lifetime in this phase quite short. Therefore, we have used the tracks in the adiabatic phase to determine the ambient density. For the SNRs that are not detected in X-rays, we determine an upper limit to the density.

The densities measured above are the initial density of the ISM in the vicinity of the SNR before the explosion took place and are based on an assumption of a uniform ISM. We can compare these density predictions with the H I observations of the column density. The H I survey of Brinks & Shane (1984) covered the disk of M31 with a resolution of $24'' \times 36''$. If we assume the M31 H I layer has a thickness of 700 pc (Braun 1991), we can convert the observed H I intensity at any position to the average ISM density in H I. We plot the ratio of densities determined in the two methods in Figure 2. Conversely, if we assume the X-ray density is accurate and the ISM is uniform, we can calculate an H I disk thickness from each SNR, shown in the top scale of Figure 2. We find that the X-ray–measured densities are consistently much lower than the densities predicted from the H I data.

There are a few caveats to this conclusion. Changing E_{51} significantly could make the X-ray and H I densities more consistent. However, theoretical considerations suggest that E_{51} should not vary by more than a factor of 2 or 3, which would shift the densities by only roughly a factor of 1.5. In fact, when we allow E_{51} to vary from 0.3 to 3.0 and compare the resulting tracks with the location of the known SNRs in the other Local Group galaxies, it is apparent that a value of 1.0 is most consistent with the location of the ensemble of known SNRs. The use of non-LTE models to calculate the X-ray luminosity would imply even lower values for the density, since the luminosity detection limit would drop. Choosing a different conversion from HRI counts to ergs can only increase the luminosity limit by 0.2 in $\log \Sigma_X$, with a corresponding increase in the density. We conclude that these effects cannot completely explain the discrepancies between the H I and X-ray measurements of the ambient ISM densities.

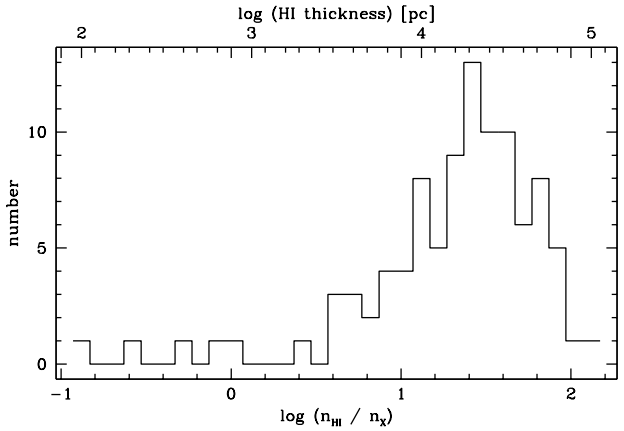

FIG. 2.—Comparison between H I column density and X-ray–measured ambient densities. The lower scale gives the logarithm of the ratio between the two density measurements, assuming the H I layer has a thickness of 700 pc. The upper scale gives the expected thickness of the H I layer, equating the H I and X-ray densities.

5. DISCUSSION

These two apparently contradictory density measurements can be reconciled if the ISM is not uniformly distributed. McKee & Ostriker (1977) presented a model for the ISM consisting of three components: the hot ionized medium (HIM) filling most of the volume (filling fraction of 0.7–0.9), the warm ionized medium (WIM) filling most of the remainder (filling fraction of ≈ 0.2), and the cold, neutral medium (CNM), filling only a small fraction of the volume (filling fraction $\approx 2\%$). Since that time, much observational work has gone to improving the details of this model. Observations of Hα in the Milky Way have shown the presence of diffuse ionized gas corresponding to the WIM (see, e.g., Reynolds 1989), with a temperature 5000 K $< T <$ 20,000 K. Observations of Galactic pulsar dispersion measures and Hα emission measures show that the WIM in the solar neighborhood is contained in clumps with density of ≈ 0.3 cm^{-3} and filling fraction of $\approx 8\%$ (see, e.g., Lyne, Manchester, & Taylor 1985; Reynolds 1991; for a summary, see Miller & Cox 1993). Although the observational evidence for a multicomponent ISM is strong, it is still difficult to make measurements of the relative contributions of the components beyond the local solar neighborhood because we view the Galaxy from within. This problem can be somewhat alleviated by studying external galaxies, which provide an alternative viewpoint, but there are also difficulties with this approach. For example, it is not possible to directly measure either the electron density of the ionized gas or the filling fraction, since observations of pulsar dispersion measures are impossible at these distances (Walterbos & Braun 1994). The [S II] ratio measurement of the electron density is not possible in these low-density regimes.

McKee & Ostriker (1977) discussed the evolution of an SNR in an inhomogenous region primarily filled with low-density gas and a small filling fraction of high-density clouds. They showed that at early times, the high-density clouds will evaporate quickly and enhance the interior density, but at later stages, the evolution will be dominated

by the principle low-density component. This description was used to explain the fact that the ISM density, determined from Galactic SNR X-ray observations in a similar fashion to Figure 1, decreases with the size of the remnant. We can therefore use our observations to constrain the typical density of the dominant low-density component. The densities implied by our observations (less than 0.1 cm^{-3}) are an upper limit to the density of the dominant low-density component (WIM or HIM) and are comparable to the HIM/WIM densities observed for our Galaxy. Deeper X-ray observations that can detect the fainter SNRs will in the future allow us to place stronger constraints on the density of these components and, with some model dependence, on the H I filling fraction as well.

We note that the SNRs observed may not sample the ISM in "typical" regions. On one hand, the SNRs may have preferentially occurred in regions dominated by the low-density components (i.e., WIM- or HIM-dominated regions). This is because the SNR progenitor stars have strong winds that may remove the high-density H I gas from around the star. Although the bubble produced by a single star may be too small for this effect to dominate, the SNR may be evolving in a bubble created by an association of massive stars that included the progenitor. On the other hand, the optical selections have biased against selecting SNRs in these regions. First, the [S II]/Hα ratio, used as a criterion by the SNR searches, will be reduced by the ionizing radiation from the massive, blue stars. Furthermore, the largest sample, that of Magnier et al. (1995), has explicitly avoided candidates in areas with many blue stars to reduce the contamination of the sample by H II regions. Finally, SNRs that occur in these WIM/HIM-dominated regions will have lower optical fluxes as well, so there will be some selection effect limiting their detection rate. In fact, a comparison of the locations of the identified SNRs and the locations of blue stars shows that there is no strong tenancy for the SNRs to lie very near OB associations.

We conclude that X-ray observations of extragalactic SNRs can be a powerful probe of the ISM structure. We have shown that the X-ray fluxes of most M31 SNRs are below the detection limits, which implies that the average ISM density in the vicinity of these SNRs is less than 0.1 cm^{-3}. This density is an upper limit to the density of the dominant low-density ISM component in the vicinity of these SNRs and is comparable to the HIM/WIM densities observed for our Galaxy. The implied H I density in the vicinity of these SNRs is between 10 and 100 times higher, which shows that a multicomponent ISM model such as described by McKee & Ostriker (1977) is required. Finally, we note that the range of X-ray surface brightnesses of our SNRs is not inconsistent with LMC SNR observations, even though known LMC SNRs typically have much higher X-ray surface brightnesses. Most LMC SNRs have not been discovered with optical surveys, but rather with X-ray surveys. A comparison between the Hα surface brightnesses of LMC and M31 SNRs shows that the LMC SNRs are optically brighter than those in M31 by a factor of greater than 10. This implies that the total SNR population of the LMC may be much larger than the current tally, perhaps by a factor of 10, and only deeper optical emission-line surveys will have sufficient sensitivity.

We thank Paul Hodge and Vikram Dwarkadas for comments and suggestions. We also thank the referee for important suggestions. This work was supported by NASA grant NAG-5337.

REFERENCES

Berkhuijsen, E. M. 1986, A&A, 166, 257
Blair, W. P., Kirshner, R. P., & Chevalier, R. A. 1981, ApJ, 247, 879
Bohlin, R. C., Savage, B. D., & Drake, J. F. 1978, ApJ, 224, 132
Braun, R., & Walterbos, R. 1993, A&AS, 98, 327
Braun, R. 1991, ApJ, 372, 54
Brinks, E., & Shane, W. W. 1984, A&AS, 55, 179
Fusco-Femiano, R., & Preite-Martinez, A. 1984, ApJ, 281, 593
Hamilton, A. J. S., Sarazin, C. L., & Chevalier, R. A. 1983, ApJS, 51, 115
Lyne, A. G., Manchester, R. N., & Taylor, J. H. 1985, MNRAS, 213, 613
Magnier, E. A., Prins, S., van Paradijs, J., Lewin, W. H. G., Supper, R., Hasinger, G., Pietsch, W., & Trümper, J. 1995, A&AS, 114, 215
McKee, C. F., & Ostriker, J. P. 1977, ApJ, 218, 148
Miller, W. W., & Cox, D. P. 1993, ApJ, 417, 579
Reynolds, R. J. 1989, ApJ, 345, 811
———. 1991, ApJ, 372, L17
Sedov, L. 1959, Similarity and Dimensional Methods in Mechanics (New York: Academic)
Walterbos, R., & Braun, R. 1994, ApJ, 431, 156
Welch, D. L., McAlary, C. W., McLaren, R. A., & Madore, B.F. 1986, ApJ, 305, 583